

Vortex and half-vortex dynamics in a nonlinear spinor quantum fluid

Lorenzo Dominici,^{1,2*} Galbadrakh Dagvadorj,³ Jonathan M. Fellows,³ Dario Ballarini,¹ Milena De Giorgi,¹ Francesca M. Marchetti,⁴ Bruno Piccirillo,⁵ Lorenzo Marrucci,⁵ Alberto Bramati,⁶ Giuseppe Gigli,^{1,2} Marzena H. Szymańska,^{7*} Daniele Sanvitto¹

2015 © The Authors, some rights reserved; exclusive licensee American Association for the Advancement of Science. Distributed under a Creative Commons Attribution NonCommercial License 4.0 (CC BY-NC). 10.1126/sciadv.1500807

Vortices are archetypal objects that recur in the universe across the scale of complexity, from subatomic particles to galaxies and black holes. Their appearance is connected with spontaneous symmetry breaking and phase transitions. In Bose-Einstein condensates and superfluids, vortices are both point-like and quantized quasiparticles. We use a two-dimensional (2D) fluid of polaritons, bosonic particles constituted by hybrid photonic and electronic oscillations, to study quantum vortex dynamics. Polaritons benefit from easiness of wave function phase detection, a spinor nature sustaining half-integer vorticity, strong nonlinearity, and tuning of the background disorder. We can directly generate by resonant pulsed excitations a polariton condensate carrying either a full or half-integer vortex as initial condition and follow their coherent evolution using ultrafast imaging on the picosecond scale. The observations highlight a rich phenomenology, such as the spiraling of the half-vortex and the joint path of the twin charges of a full vortex, until the moment of their splitting. Furthermore, we observe the ordered branching into newly generated secondary couples, associated with the breaking of radial and azimuthal symmetries. This allows us to devise the interplay of nonlinearity and sample disorder in shaping the fluid and driving the vortex dynamics. In addition, our observations suggest that phase singularities may be seen as fundamental particles whose quantized events span from pair creation and recombination to 2D+*t* topological vortex strings.

INTRODUCTION

Vortices and topological excitations play a crucial role in our understanding of the universe, recurring in the fields of subatomic particles, quantum fluids, condensed matter, and nonlinear optics and being involved in fluid dynamics and phase transitions ranging up to the cosmologic scale (1). Space-time could be seen as an analog of a superfluid (2) and elementary particles as an analog of the excitations of a medium called the quantum vacuum (3). In this sense, the phase singularities (that is, vortices) of a quantum fluid (for example, of a superfluid) are point-like and quantized quasiparticles. Here, we use a specific experimental “quantum interface”: polariton condensates (4), which are bosonic hybrid light-matter particles consisting of strongly coupled excitons and photons. The ± 1 spin components of the excitons couple to different polarization states of light, making the Bose-degenerate polariton gas a spinor condensate. The realization of exciton polariton condensates in semiconductor microcavities (5, 6) has paved the way for a prolific series of studies into quantum hydrodynamics in two-dimensional systems (7–13). Microcavity polaritons are particularly advantageous systems for the study of topological excitations in interacting superfluids, thanks to the stronger nonlinearities and peculiar dispersive and dissipative features, with respect to both atomic condensates and nonlinear optics.

Within condensates and quantum fluids, we have to distinguish between two different kinds of vortices: (i) fluctuation-generated vortex-

antivortex (V-AV) pairs, as, for example, in the Berezinsky-Kosterlitz-Thouless (BKT) transition (14, 15). These are vortices that are generated by quantum or thermal fluctuations. They appear only close to the transition, that is, where the condensate density is low and fluctuations dominate. Those are random and would most likely be washed out when averaging over multiple events. (ii) Hydrodynamic or “mean-field” vortices can appear even in a strong condensate with large coherent density due to, for example, an interplay of inhomogeneity, finite size, and drive or being directly injected by an external pulse (16). These vortices are deterministic and are not very sensitive to noise. They are determined by the strong condensate profile, for example, by the interplay of pump and disorder, which is the same between events. Averaging over repeated events does not wash them out. Here, we study the second type, or hydrodynamic vortices.

For the equilibrium spinor polariton fluid, in which the drive and decay processes are ignored, the lowest energy topological excitations have been predicted to be “half-vortices” (HVs) (17, 18). These carry a phase singularity in only one circular polarization, such that in the linear polarization basis, they have a half-integer winding number for both the phase and field direction (19). Such an excitation is complementary to a “full vortex” (FV), which instead has a singularity in each circular polarization. Even in this simplified equilibrium scenario, the question of whether HVs or FVs are dynamically stable has led to some debate (20–22) because of the presence of an inherent transverse electric–transverse magnetic (TE-TM) splitting, which often arises in semiconductor microcavities and couples HVs with opposite spin (17, 20). The issue is even more complicated in a real polariton system, which is always subject to drive and dissipation and is intrinsically out of equilibrium (23). Indeed, in the case of an incoherently pumped polariton superfluid, in contrast to the equilibrium predictions, it has been theoretically demonstrated (24) that both FV and HV are dynamically stable in the absence of symmetry breaking between the linear polarization states, whereas in its presence, only FV states are

¹Consiglio Nazionale delle Ricerche (CNR) NANOTEC, Istituto di Nanotecnologia, Via Monteroni, 73100 Lecce, Italy. ²Università del Salento, Dipartimento di Matematica e Fisica “Ennio de Giorgi,” Via Arnesano, 73100 Lecce, Italy. ³Department of Physics, University of Warwick, CV47AL Coventry, UK. ⁴Departamento de Física Teórica de la Materia Condensada, Universidad Autónoma de Madrid, 28049 Madrid, Spain. ⁵Dipartimento di Fisica, Università degli Studi di Napoli Federico II, 80126 Napoli, Italy. ⁶Laboratoire Kastler Brossel, UPMC-Sorbonne Universités, CNRS, ENS-PSL, Research University, Collège de France, 4 place Jussieu, case 74, F-75005 Paris, France. ⁷Department of Physics and Astronomy, University College London, WC1E6BT London, UK

*Corresponding author. E-mail: lorenzo.dominici@gmail.com (L.D.); m.szymanska@ucl.ac.uk (M.H.S.)

seen to be stable. On the experimental side, the first observation of spontaneous HVs in a polariton condensate was achieved under nonresonant continuous wave excitation (25), in coexistence with FVs, because of the inhomogeneous polarization splitting. The recent work of Manni *et al.* (26) shows the splitting of a spontaneously formed linear polarized vortex state (FV) into two circularly polarized vortices (HVs) under nonresonant pulsed excitation. However, also in this case, the formation and motion/pinning of these vortices are caused by strong inhomogeneities and disorder in specific locations of the sample rather than by any fundamental process intrinsic to the fluid. More complex schemes were proposed to generate lattices of many vortices by coherent multiple-spot excitation, as studied by Gorbach *et al.* (27) and Liew *et al.* (28) together with the effects of nonlinearities, and experimentally realized by use of a mask-shaped potential (29), also in the nonresonant case (30). Other structured optical pump beams were used to induce the creation of a single vortex [such as the nonresonant chiral polaritonic lenses (31)] or to directly imprint an annular chain of cowinding vortices [by shaping a resonant beam with a space light modulator (SLM) (32)]. In general, the stability of vortex states in polariton condensates remains an open issue of fundamental importance, given that the nature of the elementary excitations is likely to affect the macroscopic properties of the system such as the conditions for the BKT transitions to the superfluid state. In application, hydrodynamic polariton vortices have been proposed also for ultrasensitive gyroscopes (33) or information processing (34).

RESULTS

Experimental system

Here, we have been able to study the dynamics of HVs and FVs created into a polariton condensate in a variety of initial conditions and in a

controlled manner, taking advantage of the versatility of the resonant pumping scheme. Here, we take care to generate the polariton vortex in a specific position on the sample with sufficiently weak disorder that the biasing effects of sample inhomogeneities can be screened out for a wide range of fluid densities.

To shape the phase profile of the incoming laser beam, we use a q -plate (Fig. 1), a patterned liquid crystal retarder recently developed to study laser windings and optical vorticity (35–37). Through appropriate optical and electrical tuning, the q -plate allows us to transform a Gaussian pulse into either an FV or an HV, according to the simplified schemes shown in Fig. 1, A and B. One advantage of a q -plate over using a typical SLM is evident in the fact that the latter device works for a given linear polarization and two SLMs are needed to create an HV. The simplicity and tunability of our scheme for the resonant generation of a single polariton vortex (which can be studied in its fundamental aspects) is also advantageous over the use of a more complex multiple-spot scheme, where interference only allows for the generation of vortex lattices (28) (for example, a different system where vortex interactions play a role). In our case, the exciting pulse is sent resonant on the microcavity sample to directly create a polariton fluid carrying either an FV or HV, as shown by the emission maps in Fig. 1, C and D. Using a time-resolved digital holography (38–40) technique for the detection, we measure both the instantaneous amplitude and phase of the polariton condensate (41) in all its polarization components. Each phase singularity can be digitally tracked to record the evolution of the resonantly created vortices after the initial pulse has gone but before the population has decayed away. The lifetime of the 2D polariton fluid in our microcavity sample (42, 43) kept at 10 K is 10 ps, and we excite it by means of an 80-MHz train of 4-ps laser pulses resonant with the lower polariton energy at 836 nm.

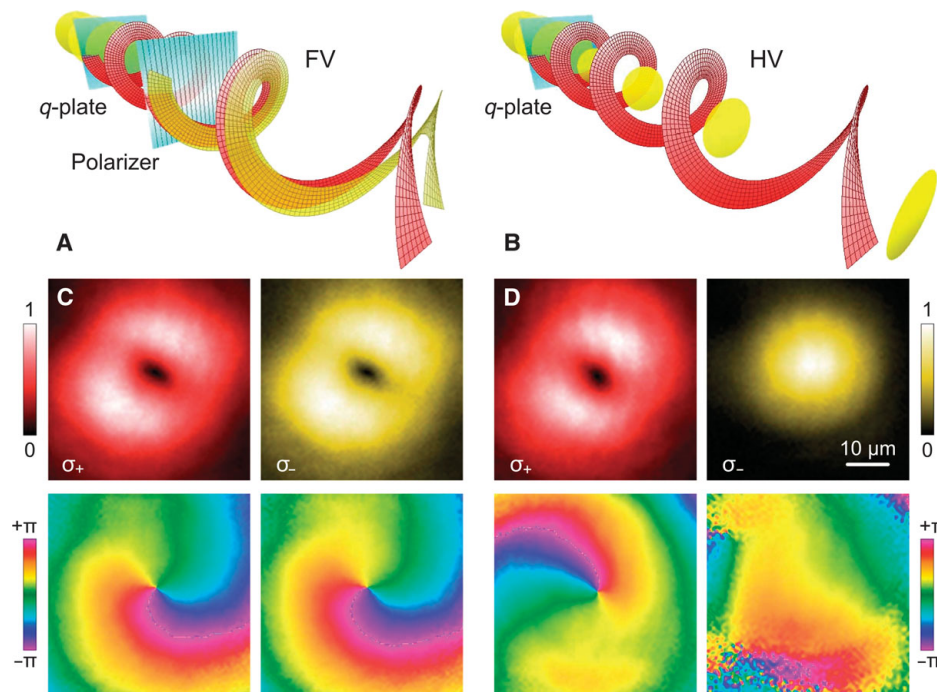


Fig. 1. Generation of optical and polariton FVs and HVs. (A and B) Experimental scheme for creation of optical FV (A) and HV (B) state via a q -plate. The disks and helices represent the isophase surfaces for Gaussian and vortex beams, respectively, in the radial regions of larger intensity. Red and yellow refer to the σ_+ (σ_-) circular polarizations. (C and D) Emission density of the polariton fluid at the time of initial generation and the corresponding phase maps.

Dynamics of HV and FV

The creation of an HV is shown in Fig. 2 at different pulse powers. In Fig. 2, A and B, the trajectory of the primary vortex ($\Delta t = 5$ to 15 ps, $\delta t = 0.5$ ps) is superimposed to the amplitude map of the opposite spin (taken at $t = 15$ ps). For both powers, the singularity of the primary HV is seen moving along a circular trajectory around the density maximum of the counterpolarized Gaussian state, keeping itself orbiting during a few tenths of picoseconds. Such curves are better depicted in Fig. 2, C and D, which are the xyt trajectories ($\Delta t = 5$ to 40 ps, $\delta t = 0.5$ ps) relative to cases in Fig. 2, A and B, respectively, and in Fig. 2E reporting the angle θ and distance d between the primary HV core and the Gaussian center of mass (see also movie S1).

The orbital-like trajectories suggest the presence of interactions between the vortex of σ_+ polaritons and the opposite σ_- density. Such dynamical configuration resembles the metastable rotating vortex state, predicted by Ostrovskaya *et al.* (44) and Gautam (45), supported by a harmonic trap, although this effective potential is dynamically modified by the intraspin repulsive forces, for example, by the deformation of the initial Gaussian. Indeed, the nonlinearities induce a breaking of radial symmetry, with the formation of circular ripples in the density. The dark ripple shown in Fig. 2B relative to the σ_- Gaussian component presents a π -jump in the phase (Fig. 2F), which is a signature of a self-induced ring dark soliton (RDS), considered its nonlinear drive. It is known that RDSs are possible solutions of a 2D fluid with repulsive interactions (42, 46, 47). Whereas intraspin interactions in an exciton polariton fluid are repulsive, interspin interactions are supposed to be attractive, with a value set by the microcavity-exciton detuning (48), and showing a possible inversion of their sign throughout resonance with a biexciton level (49). A systematic study of the vortex dynamics versus the microcavity detuning goes beyond the fundamental scope of our work. Yet, the displacement of the singularity (density minimum) with respect to the centroid (opposite spin maximum) is consistent with attractive interspin forces. This is the first time that the manifestation of opposite spin interactions in polariton condensates is directly observed through their fluid dynamic effects. We also suppose that attractive interspin forces could have some role in keeping together the twin cores of an FV at large densities, as shown in the following.

In Fig. 3, we show the generation of a vortex with winding number $l = 1$ for each circular polarization (that is, an FV) that can then be detected separately. Panels (A) to (C) represent the amplitude maps of one population (σ_+) at $t = 20$ ps with superposition of the vortex positions [trajectories for (A) and (B); instant positions for (C)] for three increasing pulse powers. The evolution of the primary singularities has been shown using 3D plots, that is, xyt curves, in panels (D) to (F) corresponding to (A) to (C), respectively. In the linear regime, at which the polariton density is low [(A) and (D) and movie S2], the opposite polarization vortices evolve jointly for the first few picoseconds once the pulse has gone. As the density starts to drop, the vortex cores show an increasing separation in space (Fig. 3G, orange), adopting independent trajectories. This suggests that the FV state is not intrinsically unstable, although it may undergo splitting supposedly driven by the sample disorder; this is triggered when the density decreases below a critical value.

At larger polariton densities (Fig. 3, B and E, and movie S3), at which the disorder is expected to be screened out, the twin singularities of the injected FV move together while the fluid is reshaped under the drive of the nonlinear interactions and the increase of radial flow. Here, they also undergo a spiraling similar to the HV case. The twin cores appear to follow the same initial path (see also Fig. 3G, violet),

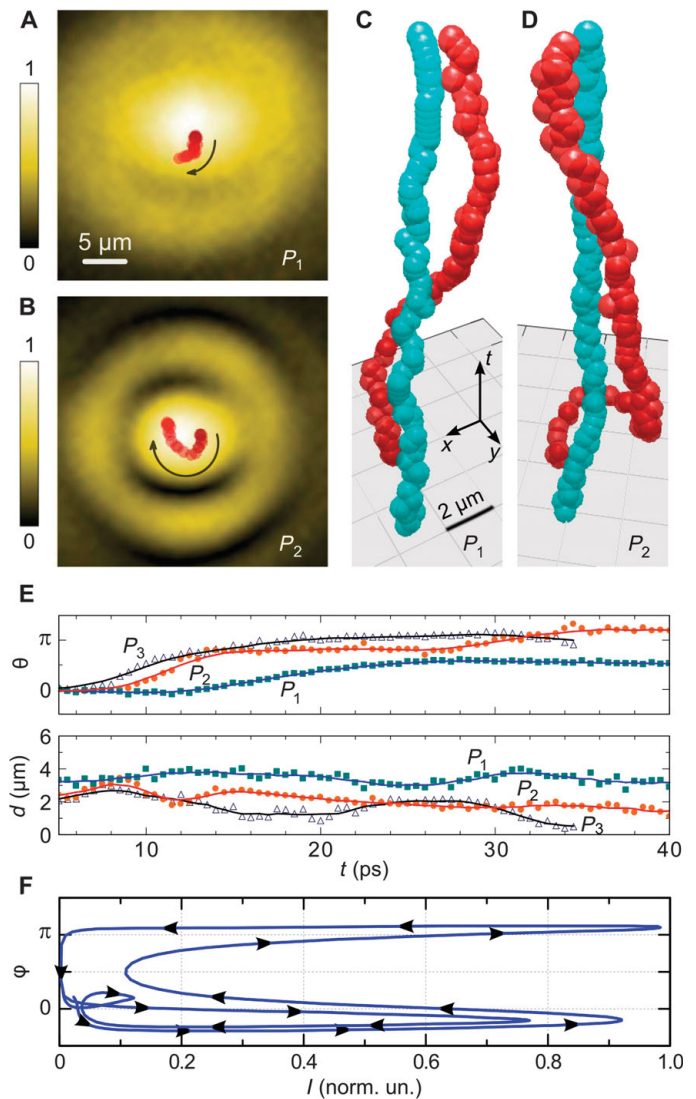


Fig. 2. Evolution of the main singularity upon HV injection. (A and B) Gaussian map together with the core trajectory in the opposite σ , both 15 ps into the evolution, at the power of $P_1 = 0.77$ mW (A) and $P_2 = 1.8$ mW (B) (see also movie S1 for power P_1). (C and D) Complete xyt vortex trajectories (time range $\Delta t = 5$ to 40 ps, time step $\delta t = 0.5$ ps) are shown for P_1 (C) and P_2 (D), with the blue spheres representing the Gaussian centroid and the red ones representing the phase singularity. (E) Angle θ and distance d between the HV core and the opposite spin centroid represented for three different powers. (F) Phase-intensity plot along a vertical cut for P_2 and $t = 22$ ps (arrows follow y), highlighting π -jumps in the phase between adjacent maxima (that is, when crossing the dark ring). norm. un., normalized units.

hence indicating the lack of any intrinsic tendency of the FV state to split. This is confirmed by increasing the polariton density further [Fig. 3, C, F, and G (cyan)], where the twin cores remain together for even longer times. Any potential instability of an FV, and the consequent tendency to split into two HVs, is not observed here, different from what was observed by Manni *et al.* (26), where the splitting after nonresonant pumping was due to marked sample inhomogeneities. On the contrary, our results show that at high densities, for which the internal currents should prevail, there is a strong inclination for the system to keep the FV

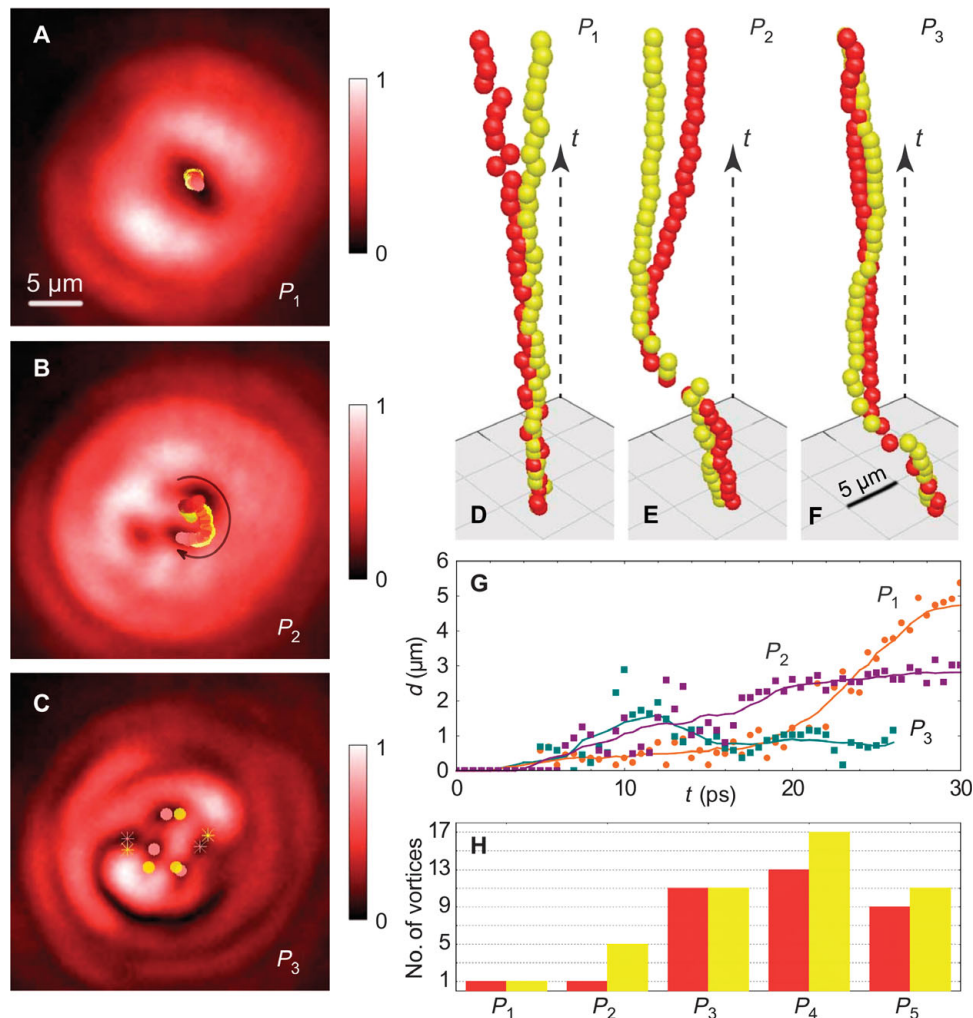


Fig. 3. Evolution of the twin singularities upon FV injection. (A to C) σ_+ density at $t = 20$ ps with superimposed phase singularities for both polarizations, marked by symbols (circle for V, star for AV, and color for spin) (see movies S2 to S4). (D to F) Trajectories of the primary vortices plotted as 3D curves xyt (time range $\Delta t = 5$ to 26 ps, time step $\delta t = 0.5$ ps) (see movie S5 for P_1). (G) Evolution in time of the intercore distance for the three cases of the previous panels. (H) Proliferation of secondary pairs (at $t = 30$ ps) upon increasing pump power. The used laser powers are $P_{1-5} = 0.17, 0.77, 1.8, 3.1,$ and 4.4 mW, which correspond to an initial excitation of $0.2, 1.0, 1.8, 2.2,$ and 2.6×10^6 total polaritons, respectively.

state together. However, note that the increased density also causes circular density ripples for the ring distribution associated with a vortex, which appear because of nonlinear radial push. This leads to the proliferation of V-AV pairs in both polarizations. In particular, secondary vortices nucleate in the low-density regions of those circular ripples (Fig. 3, C and H), which additionally disrupt the original vortex core (see also movie S4).

Theoretical modeling

To get a better understanding of the experimental vortex dynamics and interactions between the fundamental excitations, we have performed numerical simulations. The theoretical analysis performed by Rubo and collaborators (17) is based on the minimization of the total energy for an equilibrium polariton condensate of infinite size, that is, where the density profile far from the vortex core is homogeneous. This analysis allows to establish a phase diagram for the stability/instability of different vortex excitations. In contrast, here, we study the dynamics of finite-size FV and HV states and their stability during the dissipative and non-

linear evolution of interacting spinorial components, by dynamical simulations. We consider generalized dissipative Gross-Pitaevskii equations for coupled two-component excitons $\psi_{\pm}(x,y,t)$ and microcavity photon $\phi_{\pm}(x,y,t)$ fields

$$\begin{aligned}
 i\hbar \frac{\partial \psi_{\pm}}{\partial t} &= \left(-\frac{\hbar^2}{2m_{\psi}} \nabla^2 - i\frac{\hbar}{\tau_{\psi}} \right) \psi_{\pm} + \frac{\hbar\Omega_R}{2} \phi_{\pm} + \alpha_1 |\psi_{\pm}|^2 \psi_{\pm} + \alpha_2 |\psi_{\mp}|^2 \psi_{\pm} \\
 i\hbar \frac{\partial \phi_{\pm}}{\partial t} &= \left(-\frac{\hbar^2}{2m_{\phi}} \nabla^2 - i\frac{\hbar}{\tau_{\phi}} \right) \phi_{\pm} + \frac{\hbar\Omega_R}{2} \psi_{\pm} + D(x,y) \phi_{\pm} + \\
 &\quad \chi \left(\frac{\partial}{\partial x} \mp i \frac{\partial}{\partial y} \right)^2 \phi_{\mp} + F_{\pm}
 \end{aligned} \tag{1}$$

To reproduce the experimental conditions, we introduce a disorder term $D(x,y)$ for the photon field to match the inhomogeneities of the cavity mirror. The potential $D(x,y)$ is a Gaussian correlated potential

with an amplitude of strength of $50 \mu\text{eV}$ and a $1\text{-}\mu\text{m}$ correlation length. Because the effective mass of the excitons, m_{ex} , is four to five orders of magnitude greater than that of the microcavity photons, m_{ph} , we may safely neglect the kinetic energy of the excitons. The parameters in Eq. 1 are set to reproduce the experimental conditions, with exciton and photon lifetimes of $\tau_{\text{ex}} = 1000 \text{ ps}$ and $\tau_{\text{ph}} = 5 \text{ ps}$, respectively, a Rabi coupling $\hbar\Omega_{\text{R}} = 5.4 \text{ meV}$, and the exciton-exciton interaction strength $\alpha_1 = 2 \mu\text{eV} \cdot \mu\text{m}^2$. We take the strength of the interspin exciton interaction to be an order of magnitude weaker than the intraspin interaction (50), so that $\alpha_2 = -0.1\alpha_1$. The coupling between different polarizations is given by the interspin interaction α_2 and by the TE-TM splitting term χ . Following Hivet *et al.* (51), we fix the ratio between the two effective masses $m_{\text{ph}}^{\text{TE}}/m_{\text{ph}}^{\text{TM}}$ to 0.95 to have an intermediate TE-TM splitting

$$\chi = \frac{\hbar^2}{4} \left(\frac{1}{m_{\text{ph}}^{\text{TE}}} - \frac{1}{m_{\text{ph}}^{\text{TM}}} \right) = 0.026 \times \frac{\hbar^2}{2m_{\text{ph}}}$$

The initial laser pulse is modeled as a pulsed Laguerre-Gauss F_{\pm}

$$F_{\pm}(\mathbf{r}) = f_{\pm} r^{|\ell_{\pm}|} e^{-\frac{r^2}{2\sigma_r^2}} e^{i\ell_{\pm}\theta} e^{-\frac{(t-t_0)^2}{2\sigma_t^2}} e^{i(\mathbf{k}_p \cdot \mathbf{r} - \omega_p t)}$$

where the winding number of the vortex component in the \pm polarization is ℓ_{\pm} . The strength f has been selected to replicate the observed total photon output. The σ_r and σ_t parameters were chosen to have space width and time duration (full width at half maximum) of the pump $20 \mu\text{m}$ and 4 ps , respectively, in line with the experimental settings. The pump is slowly switched on into the simulation, reaching its maximum at $t_0 = 5.5 \text{ ps}$ and cut out completely after $5 \sigma_t$ to avoid any unintended phase locking. We follow the dynamics of both FVs and HVs shined resonantly with the lower polariton dispersion at $\mathbf{k}_p = 0$.

Our simulations show that only in the presence of the disorder term the imprinted vortex excitations undergo an erratic movement, both in the HV and FV configurations. In agreement with the experiments, the separation of the FV into two HVs is observed in the simulations only in the presence of disorder. In Fig. 4, A to C, we plot the trajectories for different increasing powers P_{1-3} . The dissociation is seen at earlier times at low initial density, when the sample disorder potential is expected to play a pivotal role. At larger power, the disorder and splitting are partially screened out, and the main charges move jointly for a longer time. These results are resumed in Fig. 4D and are in a good qualitative agreement with the experimental ones of Fig. 3. Simulations without disorder show that charges are dynamically stable and immune to any internal splitting. This holds in our simulations even with artificially enlarged α_2 , confirming that any dissociation is an external rather than an intrinsic effect, at least during the polariton lifetime. In other terms, although the thermodynamics would prefer HVs, on the basis of energy minimization (17), the kinetics are too slow to observe such effect in a real system. To confirm the observations from the mean-field dynamics, for some cases, we have also performed more elaborate Wigner simulations as in the study of Dagvadorj *et al.* (14), which include fluctuations. However, because our condensate density is large, the Wigner dynamics (with fluctuations) and the mean-field dynamics give comparable results, indicating that the hydrodynamic vortices we study are deterministic, that is, averaging over noise in simulations or over shots in experiments does not wash them out.

Branching and secondary vortices

In the experiments, as already stated, at large densities both the HV and FV develop concentric ripples, and this is causing generation of second-

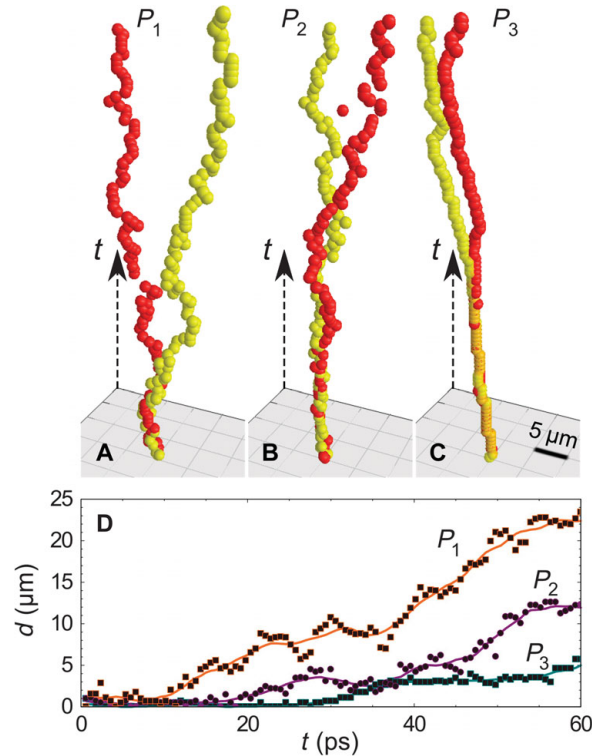


Fig. 4. Theoretical trajectories of primary singularities for FV state. (A to C) Three-dimensional (x,y,t) curves simulated at three increasing powers, with time step $\delta t = 0.4 \text{ ps}$ in a time span $\Delta t = 0$ to 60 ps . (D) Evolution of the intercore distance for the three different cases.

ary vortices. For the HV, this effect is first seen in the initially vortex-free Gaussian component, where the same amount of total polaritons are concentrated in a smaller area than in the vortex counterpart. An exemplary case of this regime is shown in Fig. 5, which reports in the first column the overlapped density maps of the two populations (red and yellow intensity scales) together with the vortices, and in the second column the σ_- phase maps. The condensate evolves from the initial time (Fig. 5A), where only the primary core of the HV is present, with the Gaussian developing more marked ripples, generating two V-AV couples (Fig. 5, B and C), which take positions in a fourfold symmetric structure (see movie S6). This effect is not driven by disorder. It is intrinsic and observed in a very large number of realizations and in different polarizations. Generation of secondary V-AV pairs is also seen in simulations where the disorder term is removed (see Fig. 7), confirming that this effect is not caused by the sample disorder. The branching dynamics and its symmetry can also be clearly seen in the 3D (xyt) trajectories of Fig. 5E (see also movie S7). The σ_+ component develops secondary pairs as well (Fig. 5D), but only at a later time (when the total population decreases substantially) and in an external region (where the density drops locally). It is worth noting that at this later stage (Fig. 5D), the primary core of the HV, which was moving around, is seen merging with a secondary vortex of the opposite polarization (but same winding), thus giving rise to the formation of an FV.

The generation of secondary vortices is also seen in case of the FV, as shown in Fig. 6, at $P = 1.8 \text{ mW}$. Panels (A) to (C) represent the joint population and vortices at different time frames, whereas the corresponding phase maps [(D) to (F)] are reported only for one polarization. We

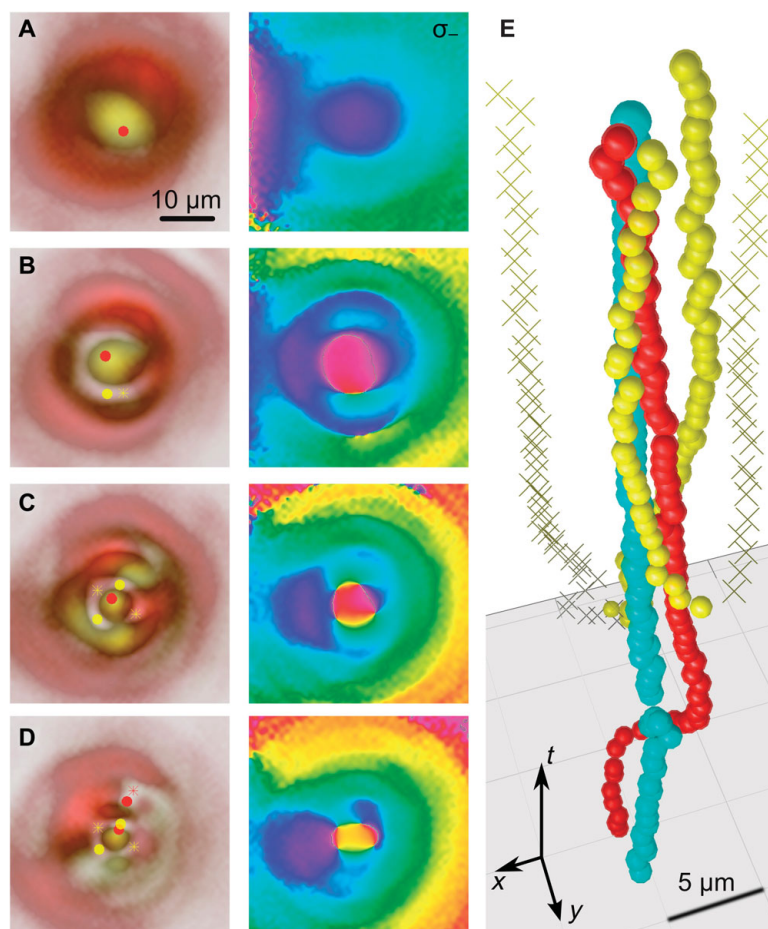


Fig. 5. Branching dynamics of an HV polariton condensate. (A to D) Four rows show frames, taken at $t = 8, 16, 24,$ and 32 ps, respectively, with densities and vortices in the first column and associated phase maps for σ_- in the second column. The initial condensate (orange due to overlap of red and yellow σ_{\pm} intensity scales) (A) undergoes the formation of concentric ripples (B to D; see also movie S6). (E) Spontaneous full V-AV formation with quadrupole symmetry for the initially Gaussian population tracked and represented as (x,y,t) vortex strings with a time step of 0.5 ps in a time span of 5 to 35 ps (see movie S7). An intermediate power (1.8 mW) was used.

observe that while the primary FV (Fig. 6A) rotates, the fluid undergoes the generation of two V-AV pairs [(B) and (C)]. The secondary pairs are created jointly between the spin populations: in other terms, the secondary topological charges are created as FV and antivortex. The σ_+ and σ_- cores of the primary and the secondary FVs move together in an FV configuration for quite a long time. The branching and its partial symmetry can also be seen in the phase maps [(D) to (F)] and in the tree structure of Fig. 6G (see movie S8), with the xyt trajectories of the vortices. At later times, the central region, initially dark, is partially filled with fluid, and some degree of asymmetry is present between the two polariton distributions. We found that at different densities, localized transient structures with three-, four-, or sixfold symmetries may also arise [see also (23)].

In the simulations, we see the emergence of density ripples (radial symmetry breaking), as observed in the experiment, above certain density (pump power) threshold, with or without the disorder. It is in the very bottom of these ripples, where the density is almost zero, that spontaneous V-AV pairs nucleate. Figure 7 shows the theoretical evolution of the density maps for the two components of an FV on each column, respectively (see also movie S9). The main difference compared with

experiments is that here the secondary couples are generated in different positions for the two polarizations. However, they keep rotating along a direction depending on their winding and not on their spins. We have reason to believe that the direction of circulation could be associated with the winding sign and the direction of the fluid reshaping (that is, contracting or expanding), but the study of such aspects is well beyond the scope of the present work.

DISCUSSION

We have used state-of-the-art excitation and ultrafast imaging techniques to investigate the dynamics and branching of quantum vortices set as initial conditions of resonantly created interacting polariton fluids. The dynamics of these topological defects is ruled by the interplay between the nonlinearity and the disorder landscape, which is modified by dissipation over time. Our main conclusion is that, surprisingly, both FV and HV are intrinsically dynamically stable, that is, the topological charges in the two spin components do not split because of intrinsic energy considerations during the lifetime of the polaritons, nor the

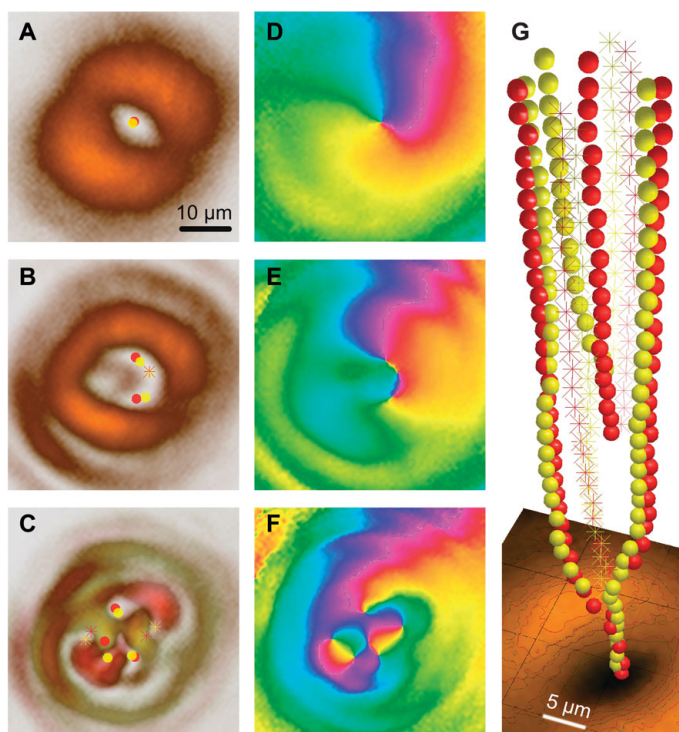


Fig. 6. Branching dynamics of an FV polariton condensate. (A to C) Density frames and vortices taken at $t = 8, 12,$ and 24 ps, respectively. (D to F) Corresponding phase maps for just one polarization (σ_-). The initial condensate [(A), orange due to overlap of red and yellow σ] develops concentric ripples (B to D); see also movie S4. (G) Spontaneous full V-AV formation tracked as (x, y, t) vortex branches with time step $\delta t = 0.5$ ps and time range $\Delta t = 6$ to 24 ps (see movie S8), for both the populations. Each secondary HV stays close to its spin counterpart until quite late into the dynamics.

singularity of an HV is seen to attract an opposite spin counterpart. We observe that the splitting effects can be attributed to the fact that at low density (long time), the fluid streamlines are affected more by the sample landscape, with disorder guiding the displacement of the vortices and eventually separating the cores when a symmetry-breaking term such as anisotropic or TE-TM splitting is at action. At intermediate-density regimes, when sample inhomogeneities are screened out and non-linear turbulence is moderate, the charges stay together for longer times. It is at even larger densities, when the main charges stay together up to tens of picoseconds, that they are also seen to move in a marked precessing trajectory, both for the HV and FV states. Here, the nonlinearities drive radial flows with the reshaping of the fluid into circular ripples of alternating high- and low-density regions, where secondary vortices nucleate. Such kind of nucleation is systematic and distinct from the proliferation of vortices at very low densities (for example, at long times or in external regions), which are pinned by disorder. This is confirmed by the theoretical simulations performed in a homogeneous landscape—the secondary charges nucleate in pairs of opposite winding in each of the two spin populations, and their evolution is seen as quasi-ordered branching of 3D ($2D+t$) singularity trees. Our observations suggest that quantum phase singularities might be seen as an analog of fundamental particles, whose features can span from quantized events such as pair creation and recombination to vortex strings. Moreover, with both

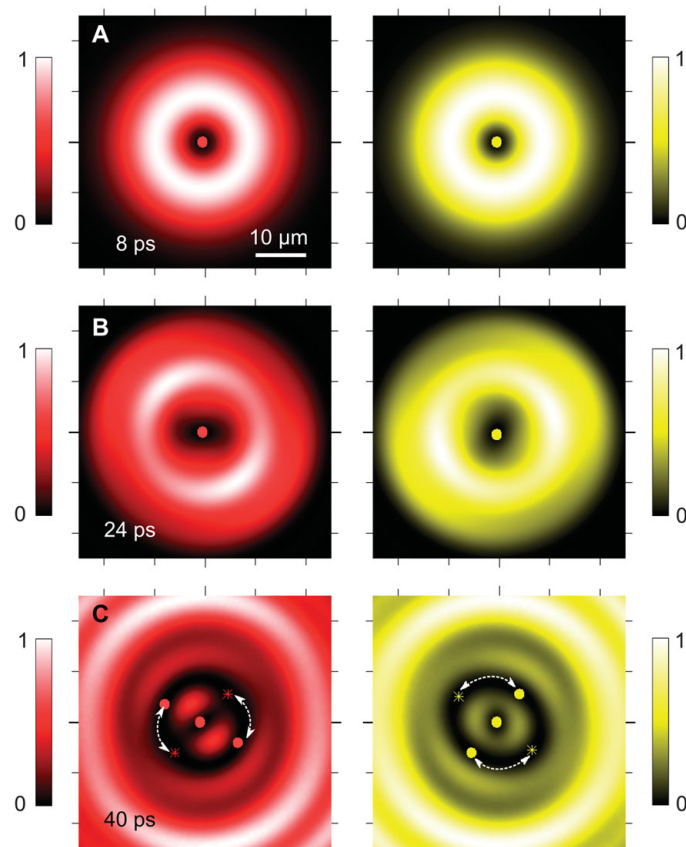


Fig. 7. Theoretical FV case without the disorder potential. (A to C) Each row corresponds to a different time: $t = 8$ (A), 24 (B), and 40 ps (C). Left and right columns represent the σ_+ and σ_- densities, respectively, with their phase singularities superimposed, marked by symbols (circle for V, star for AV, and color for spin; see also movie S9).

topological states seemingly stable during the typical polariton lifetimes, an interesting question left to be addressed is which excitations are relevant for the Kosterlitz-Thouless-type transition in these systems.

MATERIALS AND METHODS

A typical polaritonic sample was used consisting of an AlGaAs 2λ microcavity with three 8-nm $\text{In}_{0.04}\text{Ga}_{0.96}\text{As}$ quantum wells in the minima of the cavity field. Two distributed Bragg reflectors embedding the cavity, made of alternated AlAs/GaAs layers, provide an excellent quality factor ($Q = 12,000$), resulting in a lifetime for the (lower) polariton fluid of ~ 10.5 ps. All the experiments shown here are performed at a temperature of 10 K in a region of the sample clean from defects. We used an 80-MHz train of 4.0-ps laser pulses to resonantly excite the lower polaritons at ~ 836 nm and normal incidence. The phase shaping of the Gaussian pulse wavefronts is done by means of a q -plate device as illustrated in Fig. 1 and described before, to achieve an FV or HV excitation beam. On the detection side, we implemented a state-of-the-art ultrafast imaging, based on the off-axis digital holography (38–41). Its principle is to let the sample emission interfere with a delayed and coherent reference beam. This is an expanded copy of the Gaussian

excitation beam (that is, before any phase shaping) to provide a reference homogeneous in both its amplitude and phase distributions. The reference is sent to the charge-coupled device (CCD) camera with a slight angle of inclination (off-axis) with respect to the polariton emission. The obtained interferograms can be analyzed by using fast Fourier transform, in the reciprocal space, where two main informations appear. A central peak represents the sum of the time-integrated intensities of reference and emission, which can be discarded, and an off-axis modulational term, which depends on their mutual time delay. In substance, digital elaboration in the reciprocal space allows to filter only the information associated with the interference process, hence to bring back to real space the 2D snapshots of both the emission amplitude and phase, at the given time set by the delay. This allows the study of the dynamics of the polariton fluid, with spatial and temporal steps that we chose specifically as 0.16 μm and 0.5 ps, respectively. Each interferogram results from tens of thousands of repeated events because the CCD camera time is set in a range between 0.15 and 1.0 ms. The visibility of the fringes remains stable for values $\tau_{\text{CCD}} < 1.0$ ms, which cuts out the mechanical vibrations of the setup. The laser pulse fluctuations are smaller than the power variations needed to see differences in the dynamics, so that they are not affecting the averaged imaging. Additional details on the technique can be found in the study of Dominici *et al.* (41) and the supplementary material therein.

SUPPLEMENTARY MATERIALS

Supplementary material for this article is available at <http://advances.sciencemag.org/cgi/content/full/1/11/e1500807/DC1>

Movie S1. HV density map and vortex evolution (corresponding to Fig. 2A).

Movies S2 to S4. FV density maps (on a $50 \times 50\text{-}\mu\text{m}^2$ area) and twin-cores evolution at three powers (corresponding to Fig. 3, A to C).

Movie S5. FV density plus 3D *xyt* trajectory (corresponding to Fig. 3, A and D).

Movie S6. HV density and phase maps (corresponding to Fig. 5, A to D).

Movie S7. HV branching dynamics as 3D *xyt* trajectory (corresponding to Fig. 5E).

Movie S8. FV branching dynamics as 3D *xyt* trajectory (corresponding to Fig. 6G).

Movie S9. FV theoretical density and phase singularities (corresponding to Fig. 7).

REFERENCES AND NOTES

- W. H. Zurek, Cosmological experiments in superfluid helium? *Nature* **317**, 505–508 (1985).
- S. Liberati, L. Maccione, Astrophysical constraints on Planck scale dissipative phenomena. *Phys. Rev. Lett.* **112**, 151301 (2014).
- G. E. Volovik, *The Universe in a Helium Droplet* (Oxford Univ. Press, New York, 2003).
- T. Byrnes, N. Y. Kim, Y. Yamamoto, Exciton–polariton condensates. *Nat. Phys.* **10**, 803–813 (2014).
- J. Kasprzak, M. Richard, S. Kundermann, A. Baas, P. Jeambrun, J. M. J. Keeling, F. M. Marchetti, M. H. Szymańska, R. André, J. L. Staehli, V. Savona, P. B. Littlewood, B. Deveaud, L. S. Dang, Bose–Einstein condensation of exciton polaritons. *Nature* **443**, 409–414 (2006).
- R. Balili, V. Hartwell, D. Snoke, L. Pfeiffer, K. West, Bose–Einstein condensation of microcavity polaritons in a trap. *Science* **316**, 1007–1010 (2007).
- A. Dreisemann, P. Cristofolini, R. Balili, G. Christmann, F. Pinsker, N. G. Berloff, Z. Hatzopoulos, P. G. Savvidis, J. J. Baumberg, Coupled counterrotating polariton condensates in optically defined annular potentials. *Proc. Natl. Acad. Sci. U.S.A.* **111**, 8770–8775 (2014).
- G. Roumpos, M. Lohse, W. H. Nitsche, J. Keeling, M. H. Szymańska, P. B. Littlewood, A. Löffler, S. Höfling, L. Worschech, A. Forchel, Y. Yamamoto, Power-law decay of the spatial correlation function in exciton–polariton condensates. *Proc. Natl. Acad. Sci. U.S.A.* **109**, 6467–6472 (2012).
- A. Amo, S. Pigeon, D. Sanvitto, V. G. Sala, R. Hivet, I. Carusotto, F. Pisanello, G. Leménager, R. Houdré, E. Giacobino, C. Ciuti, A. Bramati, Polariton superfluids reveal quantum hydrodynamic solitons. *Science* **332**, 1167–1170 (2011).
- S. Pigeon, I. Carusotto, C. Ciuti, Hydrodynamic nucleation of vortices and solitons in a resonantly excited polariton superfluid. *Phys. Rev. B* **83**, 144513 (2011).
- D. Sanvitto, F. M. Marchetti, M. H. Szymańska, G. Tosi, M. Baudisch, F. P. Laussy, D. N. Krizhanovskii, M. S. Skolnick, L. Marrucci, A. Lemaître, J. Bloch, C. Tejedor, L. Viña, Persistent currents and quantized vortices in a polariton superfluid. *Nat. Phys.* **6**, 527–533 (2010).
- A. Amo, J. Lefrère, S. Pigeon, C. Adrados, C. Ciuti, I. Carusotto, R. Houdré, E. Giacobino, A. Bramati, Superfluidity of polaritons in semiconductor microcavities. *Nat. Phys.* **5**, 805–810 (2009).
- K. G. Lagoudakis, M. Wouters, M. Richard, A. Baas, I. Carusotto, R. André, L. S. Dang, B. Deveaud-Plédran, Quantized vortices in an exciton–polariton condensate. *Nat. Phys.* **4**, 706–710 (2008).
- G. Dagvadorj, J. M. Fellows, S. Matyjaśkiewicz, F. M. Marchetti, I. Carusotto, M. H. Szymańska, Nonequilibrium phase transition in a two-dimensional driven open quantum system. *Phys. Rev. X* **5**, 041028 (2015).
- W. H. Nitsche, N. Y. Kim, G. Roumpos, C. Schneider, M. Kamp, S. Höfling, A. Forchel, Y. Yamamoto, Algebraic order and the Berezinskii-Kosterlitz-Thouless transition in an exciton–polariton gas. *Phys. Rev. B* **90**, 205430 (2014).
- F. M. Marchetti, M. H. Szymańska, C. Tejedor, D. M. Whittaker, Spontaneous and triggered vortices in polariton optical-parametric-oscillator superfluids. *Phys. Rev. Lett.* **105**, 063902 (2010).
- M. Toledo-Solano, M. E. Mora-Ramos, A. Figueroa, Y. G. Rubo, Warping and interactions of vortices in exciton–polariton condensates. *Phys. Rev. B* **89**, 035308 (2014).
- Y. G. Rubo, Half vortices in exciton polariton condensates. *Phys. Rev. Lett.* **99**, 106401 (2007).
- G. Liu, D. W. Snoke, A. Daley, L. N. Pfeiffer, K. West, A new type of half-quantum circulation in a macroscopic polariton spinor ring condensate. *Proc. Natl. Acad. Sci. U.S.A.* **112**, 2676–2681 (2015).
- H. Flayac, I. A. Shelykh, D. D. Solnyshkov, G. Malpuech, Topological stability of the half-vortices in spinor exciton–polariton condensates. *Phys. Rev. B* **81**, 045318 (2010).
- M. Toledo Solano, Y. G. Rubo, Comment on “Topological stability of the half-vortices in spinor exciton–polariton condensates”. *Phys. Rev. B* **82**, 127301 (2010).
- H. Flayac, D. D. Solnyshkov, G. Malpuech, I. A. Shelykh, Reply to “Comment on ‘Topological stability of the half-vortices in spinor exciton–polariton condensates’”. *Phys. Rev. B* **82**, 127302 (2010).
- J. Keeling, N. G. Berloff, Spontaneous rotating vortex lattices in a pumped decaying condensate. *Phys. Rev. Lett.* **100**, 250401 (2008).
- M. O. Borgh, J. Keeling, N. G. Berloff, Spatial pattern formation and polarization dynamics of a nonequilibrium spinor polariton condensate. *Phys. Rev. B* **81**, 235302 (2010).
- K. G. Lagoudakis, T. Ostatnický, A. V. Kavokin, Y. G. Rubo, R. André, B. Deveaud-Plédran, Observation of half-quantum vortices in an exciton–polariton condensate. *Science* **326**, 974–976 (2009).
- F. Manni, K. G. Lagoudakis, T. C. H. Liew, R. André, V. Savona, B. Deveaud, Dissociation dynamics of singly charged vortices into half-quantum vortex pairs. *Nat. Commun.* **3**, 1309 (2012).
- A. V. Gorbach, R. Hartley, D. V. Skryabin, Vortex lattices in coherently pumped polariton microcavities. *Phys. Rev. Lett.* **104**, 213903 (2010).
- T. C. H. Liew, Y. G. Rubo, A. V. Kavokin, Generation and dynamics of vortex lattices in coherent exciton–polariton fields. *Phys. Rev. Lett.* **101**, 187401 (2008).
- R. Hivet, E. Cancellieri, T. Boulier, D. Ballarín, D. Sanvitto, F. M. Marchetti, M. H. Szymańska, C. Ciuti, E. Giacobino, A. Bramati, Interaction-shaped vortex-antivortex lattices in polariton fluids. *Phys. Rev. B* **89**, 134501 (2014).
- G. Tosi, G. Christmann, N. G. Berloff, P. Tsotsis, T. Gao, Z. Hatzopoulos, P. G. Savvidis, J. J. Baumberg, Geometrically locked vortex lattices in semiconductor quantum fluids. *Nat. Commun.* **3**, 1243 (2012).
- R. Dall, M. D. Fraser, A. S. Desyatnikov, G. Li, S. Brodbeck, M. Kamp, C. Schneider, S. Höfling, E. A. Ostrovskaya, Creation of orbital angular momentum states with chiral polaritonic lenses. *Phys. Rev. Lett.* **113**, 200404 (2014).
- T. Boulier, H. Terças, D. D. Solnyshkov, Q. Glorieux, E. Giacobino, G. Malpuech, A. Bramati, Vortex chain in a resonantly pumped polariton superfluid. *Sci. Rep.* **5**, 9230 (2015).
- G. Franchetti, N. G. Berloff, J. J. Baumberg, Exploiting quantum coherence of polaritons for ultra sensitive detectors. arXiv:1210.1187 (2012).
- H. Sigurdsson, O. A. Egorov, X. Ma, I. A. Shelykh, T. C. H. Liew, Information processing with topologically protected vortex memories in exciton–polariton condensates. *Phys. Rev. B* **90**, 014504 (2014).
- L. Marrucci, C. Manzo, D. Paparo, Optical spin-to-orbital angular momentum conversion in inhomogeneous anisotropic media. *Phys. Rev. Lett.* **96**, 163905 (2006).
- V. D’Ambrosio, N. Spagnolo, L. Del Re, S. Slussarenko, Y. Li, L. C. Kwek, L. Marrucci, S. P. Walborn, L. Aolita, F. Sciarrino, Photonic polarization gears for ultra-sensitive angular measurements. *Nat. Commun.* **4**, 2432 (2013).
- F. Cardano, E. Karimí, L. Marrucci, C. de Lisio, E. Santamato, Generation and dynamics of optical beams with polarization singularities. *Opt. Express* **21**, 8815–8820 (2013).
- C. Antón, G. Tosi, M. D. Martín, L. Viña, A. Lemaître, J. Bloch, Role of supercurrents on vortices formation in polariton condensates. *Opt. Express* **20**, 16366–16373 (2012).
- G. Nardin, K. G. Lagoudakis, B. Pietka, F. Morier-Genoud, Y. Léger, B. Deveaud-Plédran, Selective photoexcitation of confined exciton–polariton vortices. *Phys. Rev. B* **82**, 073303 (2010).
- U. Schnars, W. Jüptner, *Digital Holography* (Springer-Verlag, Berlin, 2005).

41. L. Dominici, D. Colas, S. Donati, J. P. Restrepo Cuartas, M. De Giorgi, D. Ballarini, G. Guirales, J. C. López Carreño, A. Bramati, G. Gigli, E. del Valle, F. P. Laussy, D. Sanvitto, Ultrafast control and Rabi oscillations of polaritons. *Phys. Rev. Lett.* **113**, 226401 (2014).
42. L. Dominici, M. Petrov, M. Matuszewski, D. Ballarini, M. De Giorgi, D. Colas, E. Cancellieri, B. S. Fernández, A. Bramati, G. Gigli, A. Kavokin, F. Laussy, D. Sanvitto, Real-space collapse of a polariton condensate. *Nat. Commun.* **6**, 8993 (2015).
43. D. Ballarini, M. De Giorgi, E. Cancellieri, R. Houdré, E. Giacobino, R. Cingolani, A. Bramati, G. Gigli, D. Sanvitto, All-optical polariton transistor. *Nat. Commun.* **4**, 1778 (2013).
44. E. A. Ostrovskaya, J. Abdullaev, A. S. Desyatnikov, M. D. Fraser, Y. S. Kivshar, Dissipative solitons and vortices in polariton Bose-Einstein condensates. *Phys. Rev. A* **86**, 013636 (2012).
45. S. Gautam, Dynamics of the corotating vortices in dipolar Bose-Einstein condensates in the presence of dissipation. *J. Phys. B* **47**, 165301 (2014).
46. A. S. Rodrigues, P. G. Kevrekidis, R. Carretero-González, J. Cuevas-Maraver, D. J. Frantzeskakis, F. Palmero, From nodeless clouds and vortices to gray ring solitons and symmetry-broken states in two-dimensional polariton condensates. *J. Phys. Condens. Matter* **26**, 155801 (2014).
47. F. Manni, K. G. Lagoudakis, T. K. Paraiso, R. Cerna, Y. Léger, T. C. H. Liew, I. A. Shelykh, A. V. Kavokin, F. Morier-Genoud, B. Deveaud-Plédran, Spin-to-orbital angular momentum conversion in semiconductor microcavities. *Phys. Rev. B* **83**, 241307 (2011).
48. M. Vladimirova, S. Cronenberger, D. Scalbert, K. V. Kavokin, A. Miard, A. Lemaître, J. Bloch, D. Solnyshkov, G. Malpuech, A. V. Kavokin, Polariton-polariton interaction constants in microcavities. *Phys. Rev. B* **82**, 075301 (2010).
49. N. Takemura, S. Trebaol, M. Wouters, M. T. Portella-Oberli, B. Deveaud, Polaritonic Feshbach resonance. *Nat. Phys.* **10**, 500–504 (2014).
50. L. Ferrier, E. Wertz, R. Johné, D. D. Solnyshkov, P. Senellart, I. Sagnes, A. Lemaître, G. Malpuech, J. Bloch, Interactions in confined polariton condensates. *Phys. Rev. Lett.* **106**, 126401 (2011).
51. R. Hivet, H. Flayac, D. D. Solnyshkov, D. Tanese, T. Boulier, D. Andreoli, E. Giacobino, J. Bloch, A. Bramati, G. Malpuech, A. Amo, Half-solitons in a polariton quantum fluid behave like magnetic monopoles. *Nat. Phys.* **8**, 724–728 (2012).

Acknowledgments: We thank G. Lerario for fruitful discussions and R. Houdré for the growth of the microcavity sample. **Funding:** We acknowledge the national project “Molecular nano-technologies for health and environment” (MAAT, PON02_00563_3316357), the Ministero dell’Istruzione dell’Università e della Ricerca project Beyond Nano, and the project European Research Council POLAFLOW (grant 308136) for financial support. M.H.S. acknowledges support from Engineering and Physical Sciences Research Council (EP/I028900/2 and EP/K003623/2). F.M.M. acknowledges financial support from the Ministerio de Economía y Competitividad, project nos. MAT2011-22997 and MAT2014-53119-C2-1-R. **Author contributions:** D.S. and M.H.S. proposed the experiment; L.D., D.S., D.B., M.D.G., and G.G. set up the experiment; L.D. supervised the experiment and analyzed the results; M.H.S., F.M.M., G.D., and J.M.F. developed the theory and the computational simulations; M.H.S. supervised the theory; A.B. provided the sample; L.M. and B.P. provided the q -plate and the know-how on optical vortices; L.D. wrote the text; and D.S. supervised and coordinated the research. All the authors discussed the results and contributed to the manuscript. **Competing interests:** The authors declare that they have no competing interests. **Data and materials availability:** All data needed to evaluate the conclusions in the paper are present in the paper and/or the Supplementary Materials. Additional data related to this paper may be requested from L.D. at lorenzo.dominici@gmail.com and M.H.S. at m.szymanska@ucl.ac.uk.

Submitted 19 June 2015

Accepted 1 September 2015

Published 4 December 2015

10.1126/sciadv.1500807

Citation: L. Dominici, G. Dagvadorj, J. M. Fellows, D. Ballarini, M. De Giorgi, F. M. Marchetti, B. Piccirillo, L. Marrucci, A. Bramati, G. Gigli, M. H. Szymańska, D. Sanvitto, Vortex and half-vortex dynamics in a nonlinear spinor quantum fluid. *Sci. Adv.* **1**, e1500807 (2015).

Vortex and half-vortex dynamics in a nonlinear spinor quantum fluid

Lorenzo Dominici, Galbadrakh Dagvadorj, Jonathan M. Fellows, Dario Ballarini, Milena De Giorgi, Francesca M. Marchetti, Bruno Piccirillo, Lorenzo Marrucci, Alberto Bramati, Giuseppe Gigli, Marzena H. Szymanska and Daniele Sanvito

Sci Adv 1 (11), e1500807.
DOI: 10.1126/sciadv.1500807

ARTICLE TOOLS

<http://advances.sciencemag.org/content/1/11/e1500807>

SUPPLEMENTARY MATERIALS

<http://advances.sciencemag.org/content/suppl/2015/12/01/1.11.e1500807.DC1>

REFERENCES

This article cites 47 articles, 6 of which you can access for free
<http://advances.sciencemag.org/content/1/11/e1500807#BIBL>

PERMISSIONS

<http://www.sciencemag.org/help/reprints-and-permissions>

Use of this article is subject to the [Terms of Service](#)

Science Advances (ISSN 2375-2548) is published by the American Association for the Advancement of Science, 1200 New York Avenue NW, Washington, DC 20005. The title *Science Advances* is a registered trademark of AAAS.

Copyright © 2015, The Authors